



Numerical Investigation of Hazardous Gas Dispersion Over Obstacles and Residential Areas

E. Fatahian, H. Salarian, H. Fatahian*

Department of Mechanical Engineering, Nour Branch, Islamic Azad University, Nour, Iran

PAPER INFO

Paper history:

Received 10 May 2020

Received in revised form 30 June 2020

Accepted 21 July 2020

Keywords:

Gas Dispersion

Computational Fluid Dynamics

Mass Fraction

Obstacles

Turbulence

ABSTRACT

In the present study, an attempt has been made to use Computational Fluid Dynamics (CFD) in the assessment of hazardous gas dispersion over obstacles. For this aim, the accidental dispersion of hazardous gas from the hole and the effect of different parameters such as changes in inlet wind velocity, the direction of the pollutant cloud and its movement, mass fraction of gas dispersion, and the pressure distribution were numerically analyzed. The flow was assumed as three-dimensional, unsteady, turbulent, and compressible. Different turbulent models were used in modeling the gas release and the most accurate one was suggested. The numerical simulation demonstrated that the gas mass fraction increased significantly due to the sudden dispersion of the gas. The amount of gas concentration gradually decreased after the formation of pollutant clouds by moving in the horizontal direction. Moreover, gas mass fraction had decreased by increasing the height. Comparing the results revealed that the pollutant cloud did not cover the surrounding area in the wind velocity of 1 m/s. Therefore, the pollutant clouds generated in this case could not impose a threat. In higher wind velocities (3 m/s and 5 m/s), the pollutant cloud approximately covered the surrounding areas, which caused a severe threat. The maximum overpressure at the hole is 5.7 Pa for a wind velocity of 5 m/s, while the maximum negative pressure was about -7.1 Pa. The influencing radius was obtained about 9.3 m. The overpressure did not cause obvious damage to buildings but led to a slight hurt to humans.

doi: 10.5829/ije.2020.33.10a.27

1. INTRODUCTION

The hazardous gas dispersion in the environment indicates a dangerous risk for people living close to chemical plants. Because heavy gas tends to stay at a lower level and disperse at a slower pace in the atmosphere, potentially they are dangerous [1-3]. The possible release and dispersion of hazardous gas to the atmosphere are occurred due to terrorist attacks, human error, and mechanical failure, etc. [1]. Nowadays, many countries have been troubled by air pollution and haze. Natural gas gain popularity with the characteristics of high environmental benefit and social benefit. The laying of gas pipeline mileage also increases rapidly to meet the increasing demand for natural gas. At the same time, concerns about the potential towards that natural gas spill could pose have been raised [4]. Accidental dispersion of hazardous gas has been investigated by many researchers

and numerical models adapted for loss prevention targets in process and chemical industries [5,6]. Urban areas are easily involved in the gas dispersion. They are classified with complex geometry from numerous buildings. These obstacles significantly affect wind velocity because wakes, recirculation, and preferential paths can strongly complicate the scenario in simulations [7]. Mainly, numerical models for gas dispersion are characterized into three types [8], phenomenological models [9,10], integral models, and CFD models [11-13]. CFD-based tools can be used for simulation of the diverse problems in engineering [14-17] and the complex urban geometries involved to investigate the impact of multiple large obstacles on hazardous gas dispersion. Recently, implementing the CFD method to model the dispersion of gas has been more common as computers are becoming more capable and faster. Beside, CFD methods give more accurate results compared to traditional

*Corresponding Author Email: fatahianhossein@gmail.com
(H. Fatahian)

models of gas dispersion [18-20].

Pontiggia et al. [21] applied a CFD technique to analyze hazardous gas releases. They validated their CFD results with experimental data and good agreement was achieved. In their study, More precisely, a new methodology including the effects of atmospheric stratification on gas dispersion was developed. Li et al. [22] experimentally and numerically studied the release and dispersion of gas. A multi-phase model is developed and validated against available experimental data. Their model could support risk assessment. Moen et al. [23] investigated and validated different turbulence models in hazardous gas dispersion. For all cases, they concluded that standard k- ϵ and RNG k- ϵ models showed reasonable results. Han et al. [24] experimentally and numerically investigated the sulfur hexafluoride gas dispersion properties for an industrial building. The removal of sulfur hexafluoride was more effective as the air outlets and inlets were arranged on the same side of the wall. In the study of Eberwein et al. [25], for risk research with new energy carrier LNG in land transport, CFD simulations for LNG-vapor dispersion was considered. They concluded that the most effective parameter for modeling the dispersion was turbulence boundary conditions at the domain boundary. Issakhov and Omarova [26] numerically considered the dispersion and movement of pollutant emission between several houses. They found that using solid grass barriers caused to increase in the concentration of pollutants on the road. On the other hand, they significantly protected nearby houses. Michioka et al. [27] used the large eddy simulation method to analyze the impact of wind-direction fluctuation on the dispersion of gas. It was concluded that the instantaneous turbulent flow with a low-frequency was produced both with and without wind-direction fluctuation.

The present study aimed to evaluate the sudden gas dispersion around buildings from a hole intended at the ground. The novelty of the present work was an integration of gas dispersion with the subsequent formation of pollutant gas cloud consequence. For this aim, a three-dimensional CFD model was conducted. Actually, the flow characteristics, the surrounding area of obstacles, and distance between them can significantly affect the concentration distribution. Furthermore, changes in inlet wind velocity, the concentration of gas, pollutant cloud, and flow characteristics were studied in detail. In addition, the turbulence models in CFD simulations were assessed based on experimental data to select the most appropriate model for further studies.

2. MODEL DESCRIPTION and BOUNDARY CONDITIONS

In the present study, ANSYS design modeler was used to design and model the geometry. Figure 1 illustrates the

computational domain including obstacles and residential areas. A $100\text{ m} \times 75\text{ m} \times 30\text{ m}$ domain was set for the computational domain and a hole for gas dispersion with a diameter of 20 mm was assumed. The dimensions of the obstacles considered in the simulation are presented in Table 1. Defining the boundary condition is an important step in the implementation of simulations. For the inlet side, the boundary condition was considered as velocity inlet. For the up and side planes, zero flux planes were used. For the outlet, the boundary condition was assumed to pressure outlet. Furthermore, the no-slip boundary condition was considered for the lower side, buildings, and reservoirs. The mass flow inlet condition was imposed for gas dispersion.

A three-dimensional mesh was used for the computational domain (Figure 2a). Also, fine meshes were used to generate the grid for the areas which are more sensitive to have higher accuracy in computations. Also, Figure 2b demonstrates the entire and closer view of the grid, respectively.

3. NUMERICAL PROCEDURE and GOVERNING EQUATIONS

In the present work, simulations were implemented using ANSYS CFX along with the finite volume method

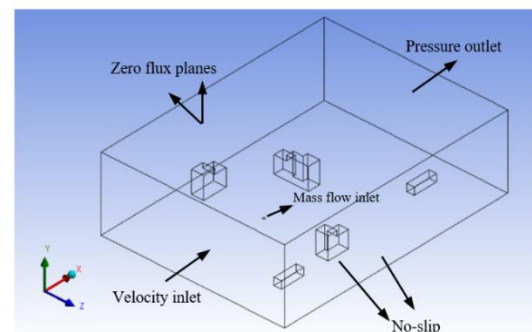


Figure 1. Computational domain

TABLE 1. The dimensions of the obstacles

Obstacles	Dimensions (m)
Reservoir 1	10×3×3
Reservoir 2	10×3×3
Building 1	5×5×9
Building 2	5×4×9
Building 3	5×5×9
Building 4	5×5×7
Building 5	5×4×9
Building 6	4×5×7
Building 7	5×5×7

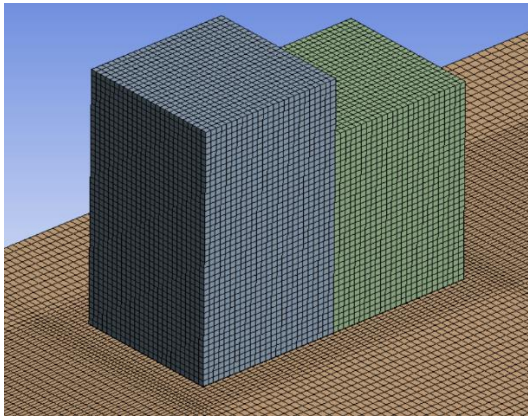


Figure 2. Computational grid for the building and ground

(FVM) to discretize the equations. Moreover, the unsteady Reynolds-Averaged Navier-Stokes (URANS) equations were adapted. Navier-Stokes Equations are solved using CFD code with specific model equations, such as energy balance, species diffusion, and turbulence which can be defined as follows:

$$\frac{\partial \rho}{\partial t} + \nabla \cdot (\rho \vec{v}) = 0 \tag{1}$$

$$\frac{\partial (\rho \vec{v})}{\partial t} + \nabla \cdot (\rho \vec{v} \vec{v}) = -\nabla p + \nabla \cdot (\vec{\tau}) + \rho \vec{g} \tag{2}$$

$$\frac{\partial (\rho C_p T)}{\partial t} + \nabla \cdot (\rho \vec{v} C_p T) = \nabla \cdot (K_T \nabla T) \tag{3}$$

where ρ represents the density, t shows the time, v denotes the velocity, p indicates the pressure, τ denotes the shear stress, g is the gravity acceleration, C_v and C_p denote the specific heats, T indicates the temperature, and k_T is the thermal conductivity.

The gas dispersion process behaves as an unsteady turbulent flow. An appropriate turbulence model is required for describing the turbulence in the gas dispersion process and make the governing equations close [28]. In this study, different turbulent models were used to select the most suitable one for further studies.

Moreover, the Upwind second-order method is used to discretize the continuity, momentum, energy, k , and ω . Also, The SIMPLE algorithm is applied for pressure-velocity coupling. The convergence criteria are considered to be less than 10^{-5} for all equations. In this study, the wind velocity at the inlet (velocity inlet boundary condition) is equal to 1, 3, and 5 m/s. For the accidental release of hazardous gas for 20 seconds, CO_2 is released at a constant mass inflow rate (m_i) of 3.65 kg/s. The variable mass inflow rate equal to m_i during the release phase (kg/s) (Q_i) is defined by a step function to enter the boundary conditions of the inlet gas (Figure 3) [29, 30]:

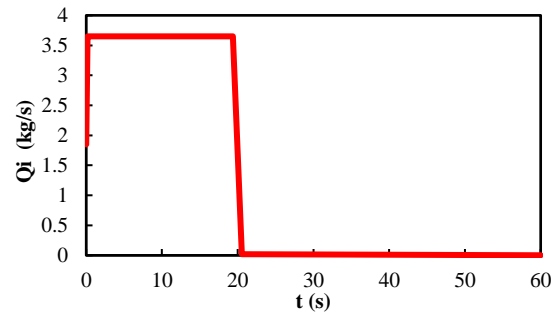


Figure 3. Q_i in terms of time (s) for the accidental release of hazardous gas

$$Q_i = m_i \times step \left[-\frac{(t-t_0)(t-t_1)}{t_c^2} \right] \tag{4}$$

where Q_i is variable mass inflow rate equal to m_i during the release phase, m_i represents the constant mass inflow rate, t denotes the time (s), t_c represents the time constant equal to 1 s, t_0 indicates the time of release initiation (s), t_1 is the release phase duration (s).

4. CODE VALIDATION

In the present study, four different grids with cell numbers of 430000, 690000, 920000, and 1050000 were generated to investigate the grid independence study using the ANSYS Meshing. The grid independence study was carried out for calculating the mass fraction of the gas dispersion along the longitudinal axis of the computational domain. Consequently, there was a negligible difference between the results of the finest grid and the grid with 920000 cells. Therefore, the grid with 920000 cells was used for selecting a favorable grid size for saving the computation time and providing better accuracy. Figure 4 indicates the detail of the grid independence study.

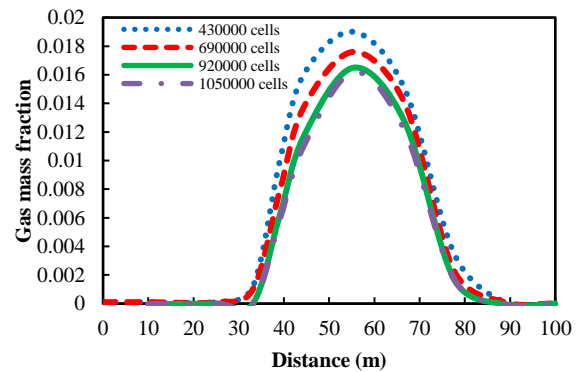


Figure 4. Grid independence study

In order to consider and choose the most appropriate turbulent model, the predicted numerical results were compared with the experimental data [29], which is shown in Figure 5. Comparing the gas concentration for different turbulent models revealed that the RNG k-ε turbulent model demonstrated better agreement with the experimental data [29]. Thus, further simulations were conducted using the RNG k-ε turbulent model.

5. RESULTS AND DISCUSSION

Figure 6 demonstrates the changes of pressure along the longitudinal axis of the computational domain for the three wind velocities of 1, 3, and 5 m/s in the x-axis direction. As it can be seen, sudden changes in pressure occurred at the gas dispersion location which has lower values at low wind velocity (1 m/s). The more changes in pressure were observed by increasing the wind velocity so that it caused a sharp increase in pressure and then significantly decreased. Finally, the pressure tends to zero at the end of the computational range for all three cases.

The maximum overpressure distributed in the center of the hole, and the overpressure gradually reduced in a radial direction. The maximum overpressure at the hole is 5.7 Pa for a wind velocity of 5 m/s, while the maximum negative pressure was about -7.1 Pa. The areas with positive and negative pressure were in dynamic change during the gas dispersion process. The influencing radius was obtained about 9.3 m. The overpressure did not cause obvious damage to buildings but led to a slight hurt to humans.

Figure 7 depicts the changes in the mass fraction of gas dispersion along the longitudinal axis of the computational domain for the three wind velocities of 1, 3, and 5 m/s. From these figures, due to the sudden dispersion of the gas, its mass fraction increased with a sharp slope. Furthermore, the amount of gas concentration gradually decreased after the formation of pollutant clouds by moving in the x-axis. It is obvious

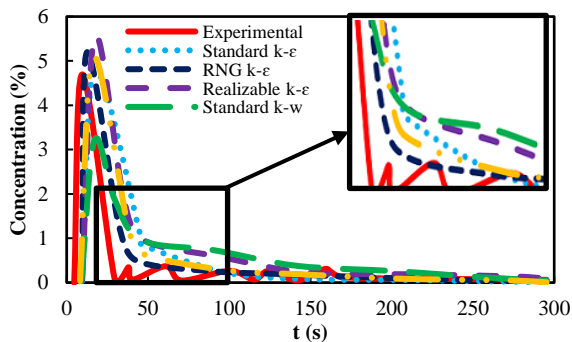


Figure 5. Comparison between gas concentrations of the present study and experimental data [29]

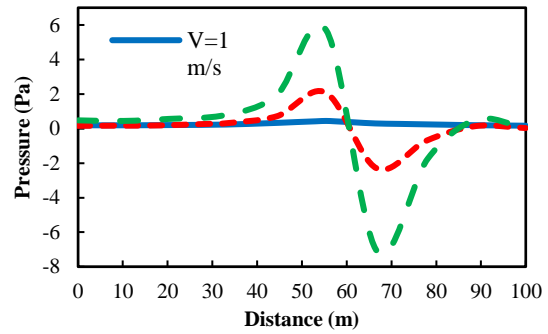


Figure 6. The changes in pressure in terms of different wind velocities

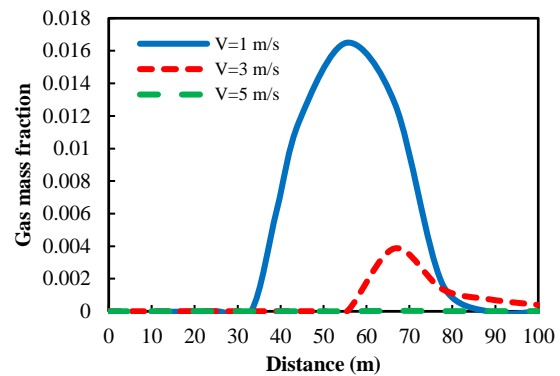


Figure 7. The changes in the gas mass fraction in terms of different wind velocities

that there is a maximum value for three cases which decreased dramatically as the wind velocity increased.

Comparing the results demonstrated that changes in wind velocity significantly affected the distribution of gas clouds. The wind is the main driving force for gas dispersion under great wind velocity [28].

The gas mainly dispersed along the vertical direction, in which the surrounding area is not covered by the gas cloud in the wind velocity of 1 m/s. Therefore, the pollutant cloud generated in this case could not impose a threat. In higher wind velocities (3 and 5 m/s), the pollutant cloud approximately covered the surrounding areas, which caused a severe threat.

The size of the coverage area depended on the pollutant cloud length. The greater pollutant cloud length was generated under the higher wind velocity. Hence, the size of the coverage area also raised with increasing wind velocity. The pollutant cloud at lower wind velocity (1 m/s) had greater gas mass fraction since the lower wind velocity cannot dissipate gas timely [28].

Figures 8 to 10 illustrate the changes in the mass fraction of dispersion gas along the longitudinal axis of the computational domain for the three wind velocities of 1, 3, and 5 m/s, and three different heights of 0, 3 and 6 m, respectively. For this purpose, three lines along the x-

axis are used, which the height of 0 m ($Y = 0$ m) means the ground surface. By considering these figures, the formation of the pollutant cloud, its concentration, and the direction of movement can be well determined. It is clear that the mass fraction of gas had decreased by increasing the height from the ground surface. It should be mentioned that with the increase of wind velocity and height, the maximum range of gas mass fraction had moved forward in the x-axis direction.

Figure 11 shows the gas concentration profile with the velocity profile at different wind velocities. From the

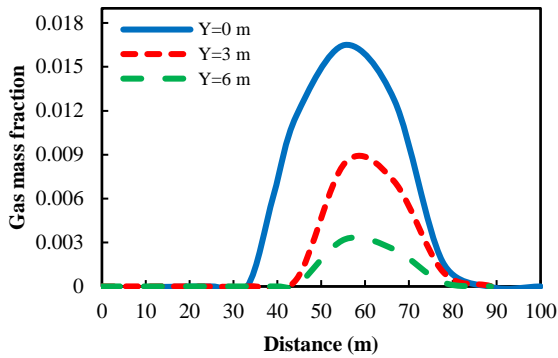


Figure 8. The changes in the gas mass fraction at $V = 1$ m/s

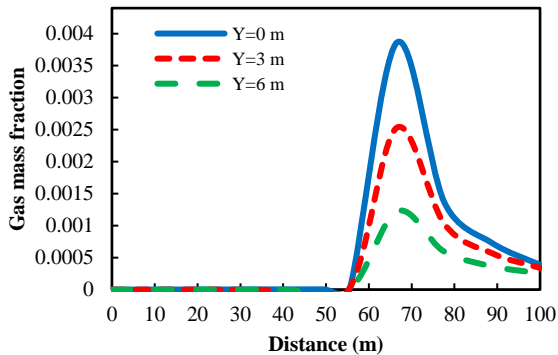


Figure 9. The changes in the gas mass fraction at $V = 3$ m/s

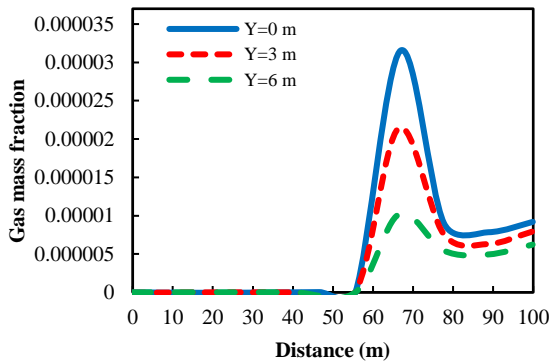


Figure 10. The changes in the gas mass fraction at $V = 5$ m/s

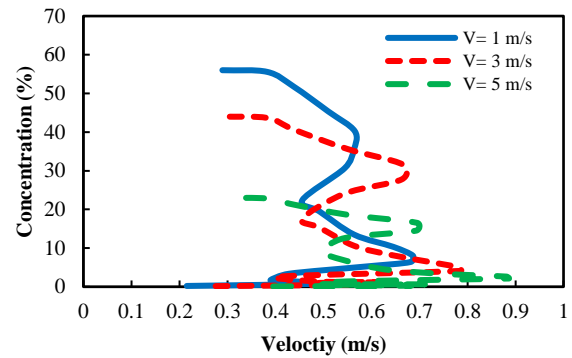


Figure 11. Gas concentration profile with the velocity profile

figures, it can be seen that a high-velocity gradient develops a turbulent flow. The sharper velocity gradient is observed with higher wind velocity. Furthermore, the gas concentration is decreased as the wind velocity increased. Whereas increasing the wind velocity from 1 m/s to 5 m/s caused the gas concentration to decrease approximately 59%.

Figure 12 illustrates the concentration fields of the x-z cross profile at the hole location and the obstacles, respectively. The instantaneous gas concentration distribution and development process of the pollutant cloud due to the incoming wind flow is clearly shown in this figure. During the initial stage of gas dispersion, the pollutant cloud with greater concentration moved along downwind in 5 s, and gradually impinged on the buildings in 15 s. After that, the majority of pollutant clouds moved upwards which caused to increase in the height of the pollutant cloud with dispersion time. Finally, the pollutant cloud completely spread and covered the surrounding areas in 35 s. It is noteworthy that the concentration of gas pollutants decreased with dispersion time whereas it tended to zero. However, the buildings should be located far enough from the threat coverage area. The influencing radius was predicted by about 11.6 m in wind velocity of 1 m/s. The high concentration of gas in this area can obviously damage humans such as pulse rate increase, nausea, headaches, and unconscious.

As mentioned earlier in Figure 7, the gas concentration decreased as wind velocity increased. This phenomenon is due to the fact that the higher wind velocity can carry more fresh air and cause faster dispersion and stronger dilution, resulting in a smaller threat area.

Figures 13 to 15 demonstrate the pressure distribution over the obstacles and residential area. It is evident that the maximum value of pressure increased as the wind velocity raised. Also, there is a high-pressure field in the locations near the buildings. There is a maximum value of pressure at the front of the buildings and a negative pressure area at the back of the buildings.

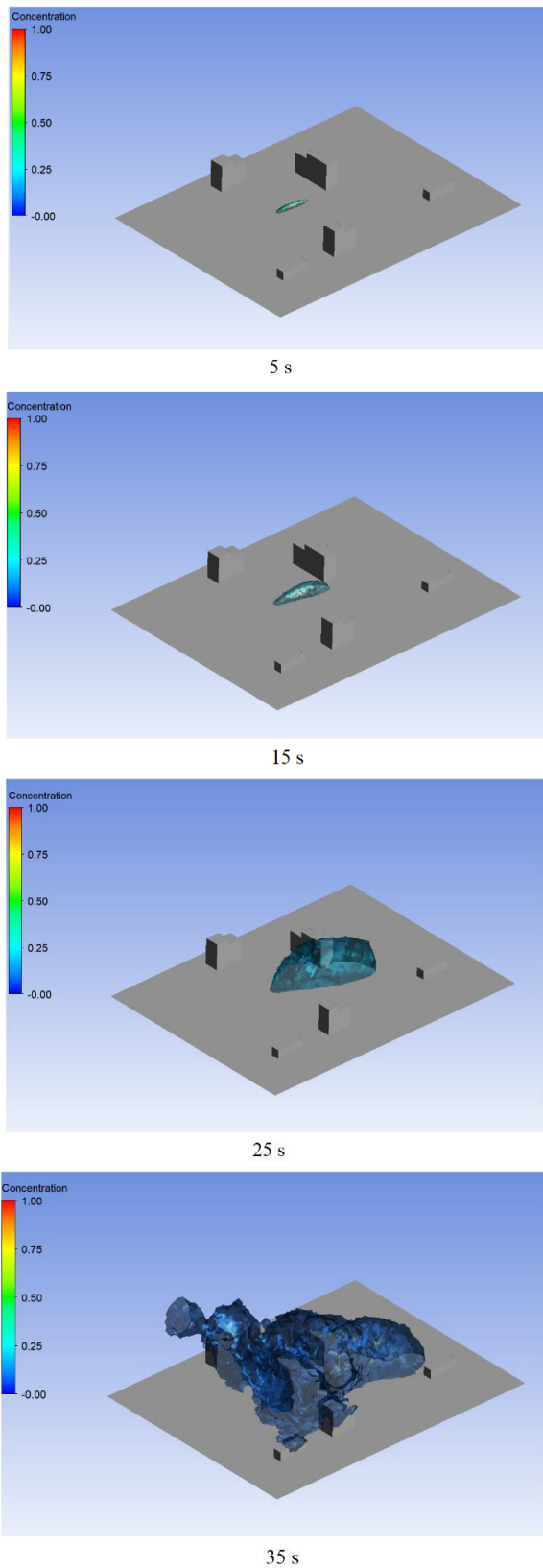


Figure 12. The development process of pollutant cloud

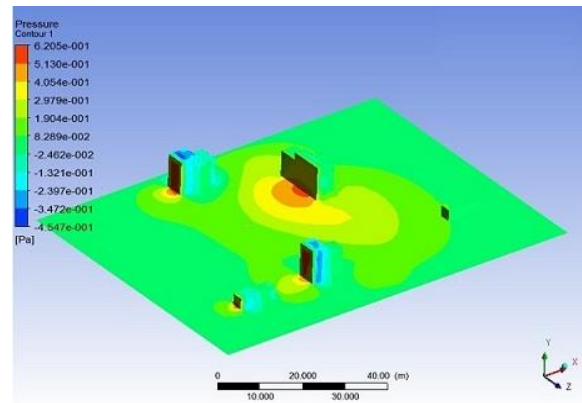


Figure 13. Pressure distribution at $V = 1$ m/s

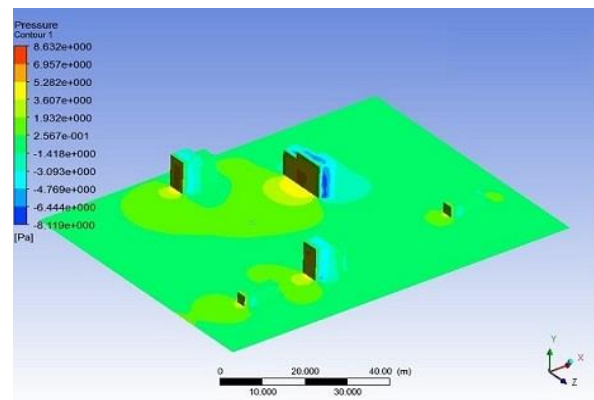


Figure 14. Pressure distribution at $V = 3$ m/s

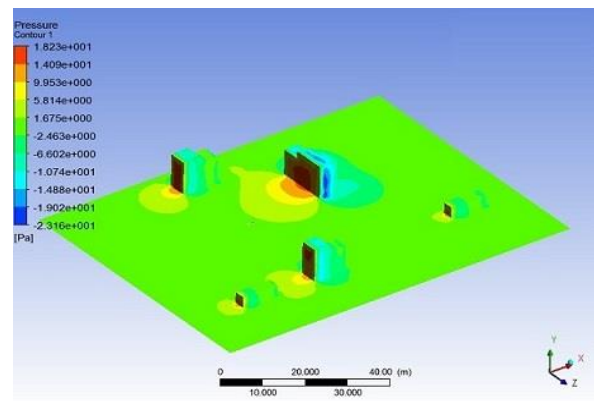


Figure 15. Pressure distribution at $V = 5$ m/s

6. CONCLUSION

In the present study, the sudden dispersion of gas from a hole intended at the ground was numerically analyzed using the CFD method. The numerical simulation was implemented using ANSYS CFX. For this purpose, a hole with a 20 mm diameter was considered and the

effects of changes inlet wind velocity, the direction of the pollutant cloud and its movement, mass fraction of gas dispersion, and the pressure distribution were studied. The flow was considered as three-dimensional, unsteady, turbulence, and compressible. The choice of turbulence model is a key in dispersion simulation using CFD codes. The results showed that the RNG k- ϵ turbulence model was suitable for simulating the gas dispersion.

The incoming wind flow carried the pollutant with high concentrations in 5 s of release and continued gradually with impingement on the buildings in 15 s. The height of the pollutant cloud increased with lower concentration which covered the surrounding areas in 35 s. Furthermore, the gas concentration decreased as wind velocity increased. This can be explained by the fact that more fresh air was carried with higher wind velocity. This resulted in faster dispersion and stronger dilution, and a smaller threat area.

7. REFERENCES

- Mirzaei, F., Mirzaei, F., and Kashi, E., "Turbulence Model Selection for Heavy Gases Dispersion Modeling in Topographically Complex Area", *Journal of Applied Fluid Mechanics*, Vol. 12, No. 6, (2019), 1745-1755. doi: 10.29252/jafm.12.06.29685
- Jiang, Y., Xu, Z., Wei, J., and Teng, G., "Fused CFD-interpolation model for real-time prediction of hazardous gas dispersion in emergency rescue", *Journal of Loss Prevention in the Process Industries*, Vol. 63, (2020), 103988. doi: 10.1016/j.jlp.2019.103988
- Liu, X., Peng, Z., Liu, X., and Zhou, R., "Dispersion characteristics of hazardous gas and exposure risk assessment in a multiroom building environment", *International Journal of Environmental Research and Public Health*, Vol. 17, No. 1, (2020), 199-210. doi: 10.3390/ijerph17010199
- Zhang, Q. X., Mo, S. J., and Liang, D., "Numerical simulation of natural gas release and risk zone forecast in urban areas", *Procedia Engineering*, Vol. 71, (2014), 470-475. doi: 10.1016/j.proeng.2014.04.067
- Zhang, Y., Wang, L., Li, A., and Tao, P., "Performance evaluation by computational fluid dynamics modelling of the heavy gas dispersion with a low Froude number in a built environment", *Indoor and Built Environment*, Vol. 29, No. 5, (2020), 656-670. doi: 10.1177/1420326X19856041
- Hanna, S. R., and Britter, R. E., *Wind flow and vapor cloud dispersion at industrial and urban sites*. John Wiley & Sons, 2010.
- Pontiggia, M., Derudi, M., Alba, M., Scaioni, M., and Rota, R., "Hazardous gas releases in urban areas: assessment of consequences through CFD modelling", *Journal of Hazardous Materials*, Vol. 1-3, (2010), 589-59. doi: 10.1016/j.jhazmat.2009.11.070
- Duijm, N. J., Carissimo, B., Mercer, A., Bartholome, C., and Giesbrecht, H., "Development and test of an evaluation protocol for heavy gas dispersion models", *Journal of Hazardous Materials*, Vol. 56, No. 3, (1997), 273-285. doi: 10.1016/S0304-3894(97)00069-1
- Britter, R. E., and McQuaid, J., HSE Contract Research Report No. 17. Workbook on the Dispersion of Dense Gases, 1988.
- Britter, R. E., "Atmospheric dispersion of dense gases", *Annual Review of Fluid Mechanics*, Vol. 21, No. 1, (1989), 317-344. doi: 10.1146/annurev.fl.21.010189.001533
- Cai, J., Chen, J., Ahmad, S., Zhao, J., Cheng, H., Zi, S., and Xiao, J., "Investigation into the effect of upstream obstacles and hazardous sources on dispersion in the urban environment with LES model", *Journal of Hazardous Materials*, Vol. 390, (2020), 121953. doi: 10.1016/j.jhazmat.2019.121953
- Hsieh, K. J., Lien, F. S., and Yee, E., "Dense gas dispersion modeling of CO₂ released from carbon capture and storage infrastructure into a complex environment", *International Journal of Greenhouse Gas Control*, Vol. 17, (2013), 127-139. doi: 10.1016/j.ijggc.2013.05.003
- Li, X., Abbassi, R., Chen, G., and Wang, Q., "Modeling and analysis of flammable gas dispersion and deflagration from offshore platform blowout", *Ocean Engineering*, Vol. 201, (2020), 107146. doi: 10.1016/j.oceaneng.2020.107146
- Eslami Afrooz, I., and Chuan Ching, D. L., "Effect of Novel Swirl Distributor Plate on Hydrodynamics of Fluidized Bed Gasifier", *International Journal of Engineering, Transactions A: Basics*, Vol. 32, No. 10, (2019), 1358-1365. doi: 10.5829/ije.2019.32.10a.04
- Rayenia, A. D., and Nassab, S. G., "Effects of Gas Radiation on Thermal Performances of Single and Double Flow Plane Solar Heaters", *International Journal of Engineering, Transactions C: Aspects*, Vol. 33, No. 6, (2020), 1156-1166. doi: 10.5829/ije.2020.33.06c.14
- Fatahian, H., Hosseini, E., and Fatahian, E., "CFD simulation of a novel design of square cyclone with dual-inverse cone", *Advanced Powder Technology*, Vol. 31, No. 4, (2020), 1748-1758. doi: 10.1016/j.appt.2020.02.007
- Fatahian, E., Salarian, H., and Fatahian, H., "A parametric study of the heat exchanger copper coils used in an indirect evaporative cooling system", *SN Applied Sciences*, Vol. 2, No. 1, (2020), 112-120. doi: 10.1007/s42452-019-1915-0
- Kashi, E., Mirzaei, F., and Mirzaei, F., "Analysis of gas dispersion and ventilation within a comprehensive CAD model of an offshore platform via computational fluid dynamics", *Journal of Loss Prevention in the Process Industries*, Vol. 36, (2015), 125-133. doi: 10.1016/j.jlp.2015.05.019
- Sun, B., Wong, J., Wadnerkar, D., Utikar, R. P., Pareek, V. K., and Guo, K., "Multiphase simulation of LNG vapour dispersion with effect of fog formation", *Applied Thermal Engineering*, Vol. 166, (2020), 114671. doi: 10.1016/j.applthermaleng.2019.114671
- Dasgotra, A., Teja, G. V., Sharma, A., and Mishra, K. B., "CFD modeling of large-scale flammable cloud dispersion using FLACS", *Journal of Loss Prevention in the Process Industries*, Vol. 56, (2018), 531-536. doi: 10.1016/j.jlp.2018.01.001
- Pontiggia, M., Derudi, M., Busini, V., and Rota, R., "Hazardous gas dispersion: a CFD model accounting for atmospheric stability classes", *Journal of Hazardous Materials*, Vol. 171, No. 3, (2009), 739-747. doi: 10.1016/j.jhazmat.2009.06.064
- Li, X., Chen, G., and Khan, F., "Analysis of underwater gas release and dispersion behavior to assess subsea safety risk", *Journal of Hazardous Materials*, Vol. 367, (2019), 676-685. doi: 10.1016/j.jhazmat.2019.01.015
- Moen, A., Mauri, L., & Narasimhamurthy, V. D., "Comparison of k- ϵ models in gaseous release and dispersion simulations using the CFD code FLACS", *Process Safety and Environmental Protection*, Vol. 130, (2019), 306-316. doi: 10.1016/j.psep.2019.08.016
- Han, O., Zhang, Y., Li, A., Li, J., Li, Y., and Liu, H., "Experimental and numerical study on heavy gas contaminant dispersion and ventilation design for industrial buildings",

- Sustainable Cities and Society*, Vol. 55, (2020), 102016. doi: 10.1016/j.scs.2020.102016
25. Eberwein, R., Rogge, A., Behrendt, F., and Knaust, C., "Dispersion modeling of LNG-Vapor on land—A CFD-Model evaluation study", *Journal of Loss Prevention in the Process Industries*, Vol. 65, (2020), 104116. doi: 10.1016/j.jlp.2020.104116
 26. Issakhov, A., and Omarova, P., "Numerical simulation of pollutant dispersion in the residential areas with continuous grass barriers", *International Journal of Environmental Science and Technology*, Vol. 17, No. 1, (2020), 525-540. 10.1007/s13762-019-02517-x
 27. Michioka, T., Takimoto, H., Ono, H., and Sato, A., "Large-eddy simulation of the effects of wind-direction fluctuations on turbulent flow and gas dispersion within a cubical canopy", *Boundary-Layer Meteorology*, Vol. 173, No. 2, 243-262, (2019). doi: 10.1007/s10546-019-00467-y
 28. Li, X., Chen, G., Zhang, R., Zhu, H., and Xu, C., "Simulation and assessment of gas dispersion above sea from a subsea release: A CFD-based approach", *International Journal of Naval Architecture and Ocean Engineering*, Vol. 11, No. 1, (2019), 353-363. doi: 10.1016/j.ijnaoe.2018.07.002
 29. Sklavounos, S., and Rigas, F., "Validation of turbulence models in heavy gas dispersion over obstacles", *Journal of Hazardous Materials*, Vol. 108, No. 1, (2004), 9-20. doi: 10.1016/j.jhazmat.2004.01.005
 30. Rice, R. G., and Do, D. D., *Applied mathematics and modelling for chemical engineers*. John Wiley & Sons, 2012.

Persian Abstract

چکیده

در مطالعه حاضر، تلاش شده است تا از روش دینامیک سیالات محاسباتی جهت ارزیابی پراکندگی گازهای خطرناک همراه با موانع استفاده شود. برای این منظور، پراکندگی تصادفی گازهای خطرناک از سطح و تأثیر پارامترهای مختلف از جمله تغییر سرعت باد ورودی، جهت ابر آلاینده و حرکت آن، کسر جرمی پراکندگی گاز و توزیع فشار به صورت عددی مورد بررسی قرار گرفته است. جریان به صورت سه بعدی، ناپایا، آشفته و تراکم پذیر فرض شده است. از مدل های توربولانسی مختلف در مدل سازی انتشار گاز استفاده شده است و دقیق ترین مدل پیشنهاد شده است. نتایج عددی نشان داده است که کسر جرمی گاز به دلیل پراکندگی ناگهانی گاز به طور قابل توجهی افزایش یافته است. با حرکت در محور افقی میزان غلظت گاز به تدریج کاهش می یابد. علاوه بر این، کسر جرمی گاز با افزایش ارتفاع کاهش یافته است. با مقایسه نتایج، مشخص شده است که ابر آلاینده در سرعت باد ۱ متر بر ثانیه محیط اطراف را پوشش نمی دهد. بنابراین، ابر آلاینده تولید شده در این حالت، نمی تواند تهدیدی را ایجاد کند. در سرعت های بالاتر باد (۳ متر بر ثانیه و ۵ متر بر ثانیه)، ابر آلاینده تقریباً مناطق اطراف را پوشانده است، که این امر تهدید قابل توجهی را ایجاد کرده است. حداکثر فشار در سوراخ ۵/۷ پاسکال برای سرعت باد ۵ متر بر ثانیه بوده است، در حالی که حداکثر فشار منفی در حدود ۰.۷- پاسکال بوده است. شعاع تأثیر گذار در حدود ۹.۳ متر بدست آمده است. فشار بیش از حد باعث ایجاد صدمات آشکار در ساختمان ها نشده است اما منجر به صدمه اندکی به انسان ها شده است.
